CCP_22

by Pranowo Pranowo

SIMULATING SEISMIC WAVE PROPAGATION IN TWO-DIMENSIONAL MEDIA USING DISCONTINUOUS SPECTRAL ELEMENT METHODS

Pranowo[a], F. Soesianto[b] & Bambang Suhendro[b]

[a] Atma Jaya Yogyakarta University, Indonesia
[b] Gadjah Mada University, Indonesia

We introduce a discontinuous spectral element method for simulating seismic wave in 2-dimensional elastic media. The methods combine the flexibility of a discontinuous finite element method with the accuracy of a spectral method. The elastodynamic equations are discretized using high-degree of Lagrange interpolants and integration over an element is accomplished based upon the Gauss-Lobatto-Legendre integration rule. This combination of discretization and integration results in a diagonal mass matrix and the use of discontinuous finite element method makes the calculation can be done locally in each element. Thus, the algorithm is simplified drastically. We validated the results of one-dimensional problem by comparing them with finite-difference time-domain method and exact solution. The comparisons show excellent agreement.

Keyword: seismic wave propagation, discontinuous spectral element, elastic media

1 Introduction

Simulation of seismic wave propagation played an important role in geophysics for imaging the structure of the earth interior and understanding the geodynamic phenomena [1]. The elastodynamic equation has been used intensively to model the seismic wave propagation in the earths. Because of analytical solutions of the equations are rare, the equations are solved numerically. The chalenge is to develop high performance numerical methods that are capable of solving the elastodynamic equations accurately and that can deal with complicated computational domain [2].

Continuous efforts have been devoted for developing numerical methods. During the last two decades, finite-difference time-domain (FDTD) methods have used extensively in modeling a large variety seismic wave propagation problems [3] [4] [5]. The FDTD methods are relatively easy to implement in computer code and do not require too much memory and CPU time. FDTD methods directly simulate the physical systems by making discrete approximation for the time and spatial derivatives via Taylor expansion to turn the partial differential equations into a system of algebraic equations. Yee introduced the first FDTD methods in 1966. This method compute electromagnetic fields that are staggered in space and time and can be interpreted as standard leapfrog method and well known as Yee's FDTD method. The Yee's FDTD methods suffer from poor numerical dispersion, which makes it difficult to run simulation for long time without introducing excessive errors and they have only second order accuracy in time and space. Some new schemes have also

started with Yee's scheme but were extended for greater accuracy rather than for geometry. High-order staggered finite-difference schemes, including compact schemes, are developed to improve the FDTD's accuracy. Pranowo et al. [6] developed multiresolution time-domain (MRTD) methods to simulate elastic wave fields. In the MRTD methods, the field components are expanded by using scaling and wavelet function then tested with using scaling and wavelet function through Galerkin's procedure. They show that computational effort can be reduced via wavelet thresholding. It is found that the implementation of MRTD on the boundaries is not easy task.

Finite volume methods (FVM), intensively used to solve fluid dynamics problems, have been adopted for elastodynamic equations [7] [1]. Le Veque [8] calculated the flux of the wave fields based Riemann solver succesfuly. Contrary to the FDTD methods, the FV methods allow one to deal with complicated geometries. The FV methods have second order accuracy and it is difficult to increase the order accuracy.

Finite element methods (FEM), based on variational formulation, can handle complicated geometries and heterogeneous material properties easily. The FE method exhibit poor dispersion properties for simulating wave propagation. Recently, least square Galerkin (LSG) [9] [10] and Discontinuous Galerkin (DG) methods [11] [12] have been developed to overcome the dispersion problems.

Spectral methods, that have high-order accuracy, have been adopted for elastodynamic equations. Spectral methods can not handle complex geometries easily. Komatitsch [13] used tensorial formulation approach for modelling curved interface. This approach can overcome the drawback, but with an increase of the computational cost.

Spectral element methods (SEM) are high-order Finite element methods which solve the variational formulations of the equations using spectral functions as basis functions. Komatistsch [2] used Legendre functions to solve the elastodynamic equations and Priolo [14] used Chebyshev functions. The Spectral element methods generate large global matrix from the elemental matrix, the methods require too much computer memory and CPU time.

In this paper we introduce a discontinuous spectral element (DSEM) method for simulating seismic wave in rectangular domain with free surface boundary conditions and internal material discontinuity. The DSEM methods combine the flexibility of a discontinuous finite element (Discontinuous Galerkin) methods with the accuracy of a spectral methods. The DSEM methods allow more general mesh (structured or unstructured mesh) configuration and inter-element continuity is not required. The basis function is discontinuous across mesh boundaries. Through a proper choices of flux computation points, the method only requires communication between mesh that have common faces. No global matrix invertion is required and the problem can be solved locally in each mesh. They are also suitable for both h- and p-type adaptivity [15] .

2 Elastodynamic Equations

Our approach of treating seismic waves numerically is based on the theory elastodynamics. We use the velocity-stress formulation as the governing equations:

$$\frac{\partial \hat{q}}{\partial t} + A \frac{\partial \hat{q}}{\partial x} + B \frac{\partial \hat{q}}{\partial y} = f \qquad (1)$$

where

$$\hat{q} = \begin{pmatrix} \tau_{xx} \\ \tau_{xy} \\ \tau_{yy} \\ v_x \\ v_y \end{pmatrix} \qquad f = \begin{pmatrix} 0 \\ 0 \\ 0 \\ f_x \\ f_y \end{pmatrix}$$

$$A = \begin{pmatrix} 0 & 0 & 0 & (\lambda + 2\mu) & 0 \\ 0 & 0 & 0 & 0 & \mu \\ 0 & 0 & 0 & \lambda & 0 \\ \dfrac{1}{\rho} & 0 & 0 & 0 & 0 \\ 0 & \dfrac{1}{\rho} & 0 & 0 & 0 \end{pmatrix} \qquad B = \begin{pmatrix} 0 & 0 & 0 & 0 & \lambda \\ 0 & 0 & 0 & \mu & 0 \\ 0 & 0 & 0 & 0 & (\lambda + 2\mu) \\ 0 & \dfrac{1}{\rho} & 0 & 0 & 0 \\ 0 & 0 & \dfrac{1}{\rho} & 0 & 0 \end{pmatrix}$$

In which v_x and v_y are the components of the velocity vector, τ_{xx}, τ_{yy} and τ_{xy} are the elements of the stress tensor and (f_x, f_y) is body force vector. The medium is described by the density $\rho(x, y)$ and the Lame coefficients $\lambda(x, y)$ and $\mu(x, y)$.

3   Discontinuous Spectral Element Methods

In this section we adopted Stanescu's notations [15] to describe the DSEM discretization. The domain is divided into non-overlapping rectangular elements within which N^{th} order Legendre polynomial (L_N) expansion is used. We mapped the global coordinates (x, y) onto local coordinates (ξ, η) in each element of the mesh. Under the mapping, equation (1) becomes

$$\frac{\partial q}{\partial t} + A \frac{\partial q}{\partial \xi} + B \frac{\partial q}{\partial \eta} = f$$

where $q = J\hat{q}$ are the transformed components of the velocity vector and stress tensor and J is the Jacobian of the transformation.

$$J = \mathbf{det}\left(\frac{\partial(x,y)}{\partial(\xi,\mu)}\right) = \Delta x \Delta y \text{ for rectangular mesh.}$$

The two-dimensional basis is constructed by taking a product of the one-dimensional basis which can be thought of as one-dimensional tensors. The one-dimensional global coordinate is transformed into elemental nodes as:

$$x_i = x_m + \frac{x_{m+1} - x_m}{2}(1 + \xi_i), i \in \{0,...,N\} \tag{2}$$

where $\Omega_m = [x_m, x_{m+1}] = \Delta x$ represents the current element, ξ_i are roots of $(1 - \xi^2)L'_N(\xi) = 0$ and L'_N denotes the derivative of L_N.
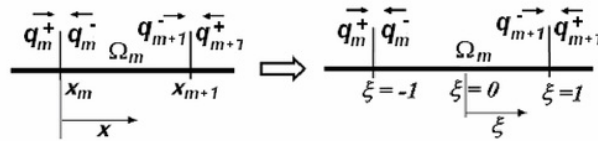
Figure 1. Local coordinate and flux.

The elemental Lagrangian interpolants $h_i(\xi)$ are chosen as a basis, it can be constructed as follows:

$$h_i(\xi) = -\frac{(1 - \xi^2)L'_N(\xi)}{N(N+1)L_N(\xi_i)(\xi - \xi_i)} \tag{3}$$

The vector q is expanded using tensor product of equation (3) as follows:

$$q(t,\xi,\mu) = \sum_{i=0}^{N}\sum_{j=0}^{N} q_{ij}(t)h_i(\xi)h_j(\eta) \tag{4}$$

where $q_{ij}(t)$ denote pointwise value of q at time t. After we sample Galerkin procedure using the same trial function within each element, we obtain the following equation:

$$\left(\frac{\partial q}{\partial t}, \phi_{ij}\right) + \left(A\frac{\partial q}{\partial \xi}, \phi_{ij}\right) + \left(B\frac{\partial q}{\partial \eta}, \phi_{ij}\right) = (f, \phi_{ij}) \tag{5}$$

We can simplified the equation (5) as:

$$\left(\frac{\partial q}{\partial t}, \phi_{ij}\right) + \left(\nabla_{\xi}\mathbf{F}, \phi_{ij}\right) = \left(f, \phi_{ij}\right) \tag{6}$$

where $\mathbf{F} = Aq\,\vec{\mathbf{i}} + Bq\,\vec{\mathbf{j}}$ is the flux vector. Here $(.,.)$ represent the usual L^2 inner product, and $\phi_{ij} = h_i(\xi)h_j(\eta)$ are the trial function. Using the divergence theorem, equation is recast as:
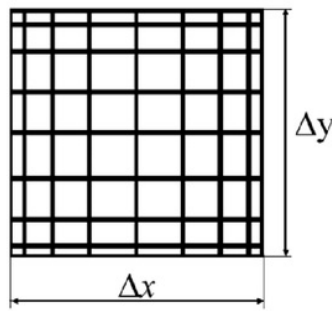
$$\left(\frac{\partial q}{\partial t}, \phi_{ij}\right) + \int_{\partial\Omega} \phi_{ij}\,\mathbf{F}\bullet\mathbf{n}\,dS = \left(\mathbf{F}, \nabla_{\xi}\phi_{ij}\right) + \left(f, \phi_{ij}\right) \tag{3}$$

where $\mathbf{n}$ is normal to the of element interface.

The Gauss-Lobatto-Legendre (GLL) quadrature is applied to integrate the integrals. The GLL quadrature is defined as follows:

$$\int_{-1}^{1} \Phi(\xi)d\xi = \sum_{i=0}^{N} \Phi(\xi_i)\omega_i \tag{4}$$

The points $\xi_0 = -1$, $\xi_N = 1$ $L'_N(\xi_i) = 0$ $\forall i \in \{1,2,...,N-1\}$ are called GLL Points, Φ is arbitrary polynomial. As long as Φ is a polynomial of degree less than $(2N-1))$ this quadrature rule is exact.

Figure 2. Element and GLL points.

After expanding the boundary integral and and performing some algebraic manipulation, we obtain the semi discrete form of the equations at the GLL points.

$$\frac{\partial q_{ij}}{\partial t} = \frac{1}{\Delta x}\left[-\mathbf{D}^{\xi}\,\mathbf{F} + \left(\frac{1}{\omega_N}\mathbf{F}^{*}\left(1,\eta_j\right)h_i\left(1\right)\right) - \frac{1}{\omega_0}\mathbf{F}^{*}\left(-1,\eta_j\right)h_i\left(-1\right)\right] +$$

$$\frac{1}{\Delta y}\left[-\mathbf{D}^{\eta}\,\mathbf{F} + \left(\frac{1}{\omega_N}\mathbf{F}^{*}\left(\xi,1\right)h_j\left(1\right)\right) - \frac{1}{\omega_0}\mathbf{F}^{*}\left(\xi,-1\right)h_j\left(-1\right)\right] + f_{ij} \tag{5}$$

Notation F^{*} denotes numerical flux at the interface between elements and it can be approximated by using average flux:

$$\mathbf{F}^{*} = \frac{1}{2}\left(\mathbf{F}^{+} + \mathbf{F}^{-}\right) \tag{7}$$

The differential matriks $\mathbf{D}$ can be written as:

$$\mathbf{D} = \frac{\partial h_j\left(\xi_i\right)}{\partial \xi}\begin{cases}\dfrac{L_m\left(\xi_i\right)}{L_m\left(\xi_j\right)\left(\xi_i - \xi_j\right)} & \text{if } i \neq j \\ 0 & \text{if } i = j, i \neq 0, m \\ \dfrac{-m\left(m+1\right)}{4} & \text{if } i = j = 0 \\ \dfrac{m\left(m+1\right)}{4} & \text{if } i = j = m\end{cases} \tag{8}$$

For simplicity, we use explicit staggered leapfrog method which has second order accuracy for temporal discretization.

4 Numerical results and discussion

4.1. One-dimensional problems

The methodology described above has been validated by comparison with both exact solution and FDTD methods for one-dimensional problem [16]. The following initial conditions are taken to perform numerical simulations:

$$v_y\left(x,0\right) = 0$$

$$\tau_{xy}\left(x,\frac{\Delta t}{2}\right) = \exp\left(-\ln 2x^2/9\right) \qquad ; -100 \leq x \leq 100$$

$$\tau_{xy}\left(x,t\right) = \left(\exp\left(-\ln 2\left(\left(x-t\right)^2\right)/9\right) + \exp\left(-\ln 2\left(\left(x+t\right)^2\right)/9\right)\right)/2 \tag{9}$$

In both DSEM and FDTD, we performance the calculations by taking

$$\Delta t = 0.05 \text{ and } CFL = 0.075, 0.01, 0.125, 0.15$$

Courant Friedrich Lewy Number CFL is calculated as

$$CFl = v \frac{\Delta t}{\Delta x} \quad \text{for FDTD}$$

and

$$CFl = v \frac{\Delta t}{\Delta x_{min}} \text{ for DSEM}$$

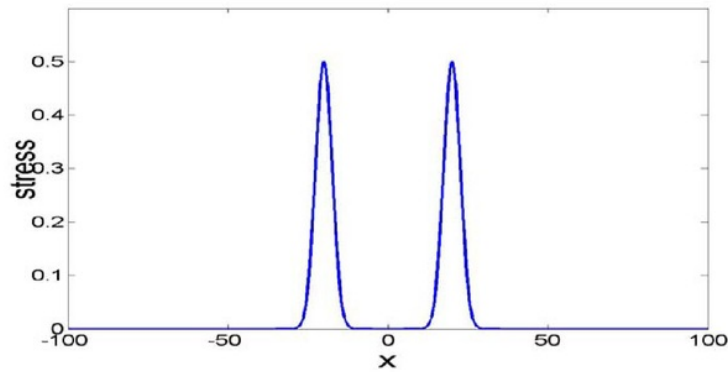For DSEM, we take fixed order of polynomial $N = 8$. Figure 3 shows the exact solution for the stress at time=20.025.

Figure 3. Exact solution for the stress at t=20.025

Since this problem has well-defined (infinitely smooth), we begin by computing the true error $\left\| \tau_{exact} - \tau_{numerical} \right\|_{\infty}$ for both DSEM and FDTD. In figure 4, the discrete maksimum error $\left\| \tau_{exact} - \tau_{numerical} \right\|_{\infty}$ is plotted versus the degrees of freedom (*dofs*). From the figure, we can see that DSEM need number of *dofs* approximately less than a half of FDTD's *dofs* to achieve the same accuracy.
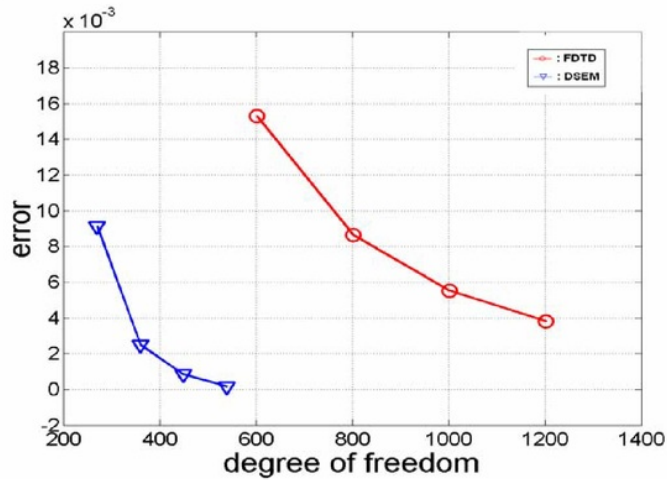
Figure 4. Comparison number of dofs between DSEM and FDTD

The accuracy of the solution in both DSM and FDTD is illustrated in figure 5 for various low CFL numbers. We can see that maksimum error $\left\| \tau_{exact} - \tau_{numerical} \right\|_{\infty}$ for DSEM decreased faster than FDTD as the CFL number increases.
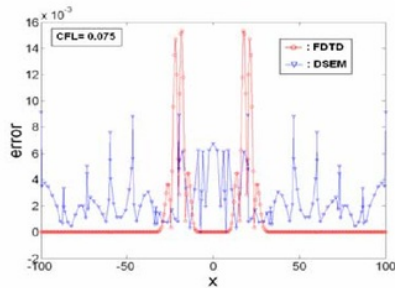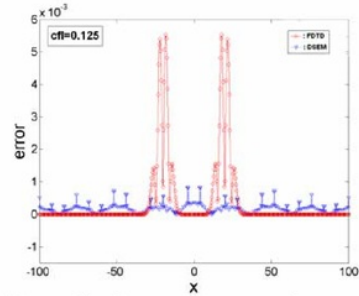

Figure 5a. Comparison error between DSEM and FDTD for CFL=0.075
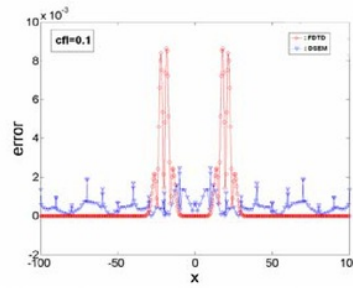
Figure 5a. Comparison error between DSEM and FDTD for CFL=0.1

High-order basis of DSEM can suppress the error of DSEM, but the use of average flux makes the error spread out in entire domain. If the basis is constant, it will make DSEM equal to central difference schemes of Finite Difference methods which are not stable. Staggered grid can reduce the error, it is shown in figure 5. The error of FDTD is localized only in region where large gradient of the fields, i.e. sharp wave front, occurs.

Figure 5c. Comparison error between DSEM and FDTD for *CFL*=0.125
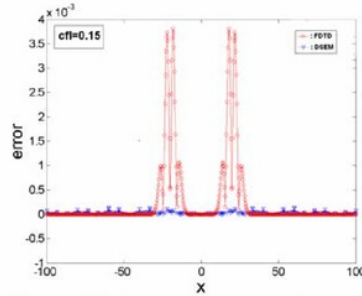
Figure 5d. Comparison error between DSEM and FDTD for *CFL*=0.15

4.1. Two-dimensional problems

The model we consider is two layered for heterogeneus media. The medium has a horizontal internal boundary that divides it into two layers. The upper layer is characterized by a P-wave velocity of 2000 m.s^{-1}, an S-wave velocity of 1300 m.s^{-1}, and a mass density of 1000 kg.m^{-2}. The lower layer elastic parameters are a P-wave velocity of 2800 m.s^{-1}, an S-wave velocity of 1473 m.s^{-1}, and a mass density of 1500 kg.m^{-2} [2]. A strong contrast both in velocity and in Poisson's ration is hence modeled, with ν =0.13 for the lower layer and ν =0.38 for the upper layer. The source is explosive and located inside the upper layer.
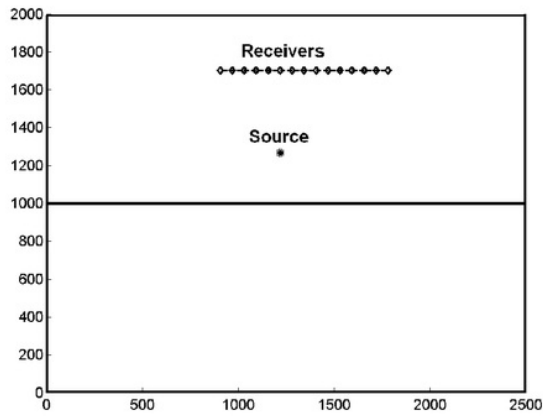
Figure 6. Two layered heteregeneous elastic media

The numerical model has a width of 2500 m amd a height of 2000 m. The source position is $(x, y) = (1218.75, 1366.67)$ m. The line of receivers goes from $x = 906.25$ m to $x = 1781.25$ m at $y = 1700$ m. The mesh is composed of 30×40 elements, with polynomial of order $N = 12$. The explosive source is a Ricker wavelet in time with central frequency of 14.5. The time step $\Delta t = 2.5$ m sec. Figure 6 shows the description of the model. The four sides of the model are assigned to be free surfaces.

Figure 7 shows the snapshots of $P - SV$ wave propagation in two-layered media at $t = 0.1875, t = 0.2625, t = 0.3375, t = 0.4125, t = 0.4875, t = 0.5625$ sec. The entire wavefields are composed of direct phases (P,S), reflected waves from internal boundary (PPr, PSr, SPr, SSr) or the free surface (PP,PS). Mode conversions of wave reflected at the internal boundary as well as at the top free surface are clearly visible.
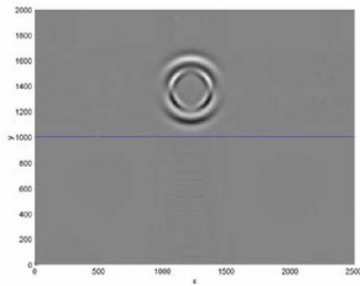
Figure 7a. τ_{yy} field at $t = 0.1875$ sec
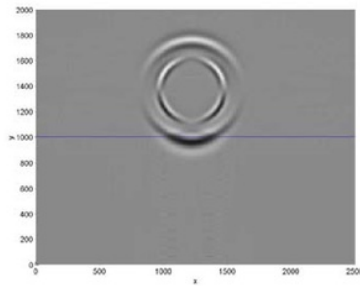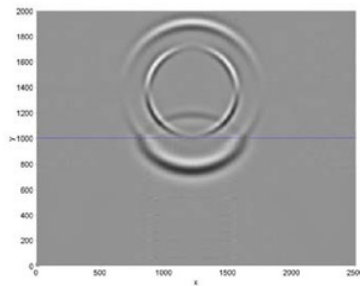

Figure 7b. τ_{yy} field at $t = 0.2675$ sec
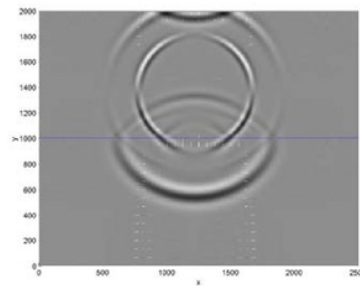

Figure 7c. τ_{yy} field at $t = 0.3375$ sec

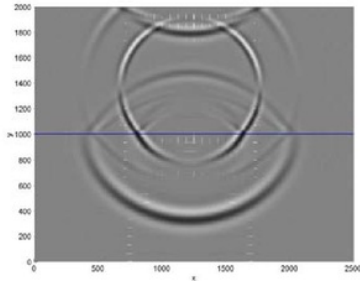Figure 7d. τ_{yy} field at $t = 0.4125$ sec

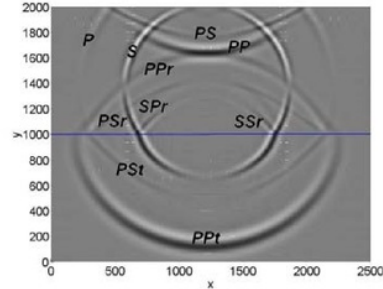Figure 7e. τ_{yy} field at $t = 0.4875$ sec

Figure 7f. τ_{yy} field at $t = 0.5625$ sec

Figure 8 shows the numerical time response of $P - SV$ waves in heterogeneous medium recorded at 15 receivers placed horizontally inside the medium.
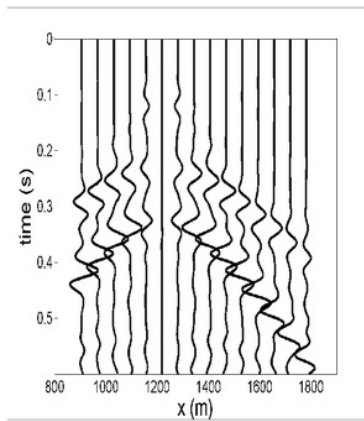

Figure 8. Seismogram of v_x

5   Conclusion

We have presented discontinuous spectral element methods for simulation of seismic wave propagation. Comparison with the FDTD methods for one-dimensional problem shows that DSEM need dofs less than FDTD methods for the same accuracy. We demonstrated that heteregeneous media, that contain material discontinuity, can be handled easily by using DSEM. Mode conversion of reflected waves can be captured well.

For future research, we plan to extend the DG method for solving problems with irregular domain and apply *hp adaptive* technique to increase the accuracy and to reduce computational costs. The numerical flux will be calculated based on Riemann solver.

Acknowledgment

References

[1] Kaser, M.A. (1999), *Simulation of seismic wave propagation on irregular grids*, Diplomarbeit, Ludwig-Maximilians-Universitat, Muenchen.

[2] Komatitsch, D. & J. P.Villote (1998), The spectral element Method: An efficient tool to simulate response of 2D and 3D geological structure , *Bulletin of the Seismological Society of America*, Vol. 2, 368-392.

[3] Virieux, J. (1986), P-SV wave propagation in heteregeneous media: velocity-stress finite difference method, *Geophysics* 51, 889-901.

[4] Meyer, T.F.N., (2001), *Numerical simulation of 3-D seismic wave propagation through subduction Zones*, Diplomarbeit, Ludwig-Maximilians-Universitat, Muenchen.

[5] Ewald, M.A, (2001), *Numerical simulation of site effects with application to the Cologne basin*, Diplomarbeit, Ludwig-Maximilians -Universitat, Muenchen.

[6] Pranowo, F. Soesianto & B. Y. Andiyanto (2003), The Multiresolution time-domain method based on Haar wavelets for numerical simulation of elastic wave propagation, *Proceedings of International Seminar on Aerospace Technology*, Yogyakarta, Indonesia.

[7] Dormy, E. & A. Tarantola (1996), Numerical simulation of elastic wave propagation using a finite volume method, J. Geophysics. Res., 100, 2123-2133.

[8] Le Veque, R.J. (2004), *Finite-Volume methods for hyperbolic problems*, Cambridge University Press, Cambridge.

[9] Thompson, L.L. (1994), *Design and analysis of space-time and Galerkin least-squares finite element methods for fluid structure interaction in exterior domain*, Ph.D thesis, Stanford University.

[10] Hulbert, G. (1989), Space-time finite element methods for second order hyperbolic equations, Ph.D thesis, Stanford University.

[11] Li, X.D. (1996), *Adaptive Finite Element Procedures in Structural Dynamics*, Ph.D Thesis, Chalmers University of Tecnology.

[12] Ekevid, T. (2003), Computational solid wave prpagation: Numerical technique and industrial applications, Ph.D. Thesis, Chalmers University of Tecnology.

[13] Komatitsch, F. Coutel & P. Mora (1996), Tensorial formulation of the wave equation for modelling curved interface, *J. Int. Geophys.*, 127, 156-168.

[14] Priolo, E. (2001), Earthquake ground motion simaulation through the 2-d spectral element method, *J. Computational Acoustics*, Vol. 9 no. 4, 127, 1561-1581.

[15] Stanescu, D., M.Y. Hussaini & F. Farassat (2002), Aircraft noise scattering – A Discontinuous spectral element approach, *Proceedings of the 40th AIAA Aerospace Sciences Meeting*, Reno, NV, USA.

[16] Pranowo, F. Soesianto & B. Suhendro (2004), High-order discontinuous galerkin for numerical simulation of elastic wave propagation, *Proceedings of Quality in Research*, Jakarta, Indonesia.

PRANOWO: Ph D student at Department of Electrical Engineering, Gadjah Mada University, Jl. Grafika 2 Yogyakarta 55281, Indonesia.
Department of Informatics, Atma Jaya Yogyakarta University.
Jl. Babarsari 43 Yogyakarta 55281, Indonesia.
E-mail: pran@mail.uajy.ac.id}

F. SOESIANTO: Department of Electrical Engineering, Gadjah Mada University, Jl. Grafika 2 Yogyakarta 55281, Indonesia.

BAMBANG SUHENDRO: Department of Civil Engineering, Gadjah Mada University, Jl. Grafika 2 Yogyakarta 55281, Indonesia.

CCP_22

Geophysical Journal International, 2006
Publication

7 Dimitri Komatitsch. "The spectral element method for elastic wave equations: Application to 2D and 3D seismic problems", SEG Technical Program Expanded Abstracts, 1999
Publication

1%

8 tel.archives-ouvertes.fr
Internet Source

1%

9 www.spice-rtn.org
Internet Source

1%

10 Gaetano Festa, Jean-Pierre Vilotte. "The Newmark scheme as velocity-stress time-staggering: an efficient PML implementation for spectral element simulations of elastodynamics", Geophysical Journal International, 2005
Publication

1%

Exclude quotes	On	Exclude matches	< 1%
Exclude bibliography	On		

CCP_22

FINAL GRADE

GENERAL COMMENTS

/0

Instructor